Enhanced bulk catalyst dissolution for self-healing materials†

Timothy C. Mauldin[a] and Michael R. Kessler*[b]

Received 25th February 2010, Accepted 11th March 2010
First published as an Advance Article on the web 12th April 2010
DOI: 10.1039/c0jm00521e

A model was developed to aid in the selection of healing monomers that can rapidly dissolve catalysts in self-healing materials. Predictions are made regarding dissolution rates of Grubbs' catalyst in a small library of ring-opening metathesis polymerization (ROMP)-active norbornenyl-based healing monomers. The Grubbs' catalyst and the healing monomers were experimentally assigned sets of Hansen parameters, and it was observed that healing monomers and blends of monomers with parameters similar to the catalyst were able to rapidly dissolve the catalyst. The model is limited in its ability to predict dissolution trends of healing monomers with substantially different viscosities.

Introduction

In the past decade, polymers and composites that can repair themselves with complete, or nearly complete, autonomy have been extensively studied in academia and received significant commercial interest.[1–3] Perhaps the most ubiquitous self-healing mechanism developed to date incorporates liquid monomer-filled vessels and catalyst particles into a polymer matrix. Upon material fracture, vessels rupture, followed by flow of the liquid monomer into the crack volume. When the monomer contacts the catalyst particles it polymerizes and adheres the crack faces together (Fig. 1).[4–7] The first and most well-studied monomer/catalyst combination used thus far in self-healing systems is dicyclopentadiene (DCPD) and Grubbs' catalyst, the former of which undergoes ring-opening metathesis polymerization (ROMP)[8–10] in the presence of the latter.[11–17] This system worked well to first demonstrate self-healing as both the catalyst and DCPD satisfy many of the unique and complex requirements of this healing mechanism, but owing to the price of Grubbs' catalyst, the research community has been slowly moving away from ROMP-based self-healing in favor of healing based on other chemistries. But while healing with these other chemistries (notably siloxane polycondensation,[18] epoxy ring-opening polymerization,[19] solvent activation of residual matrix reaction,[20] and click chemistry,[21] among others) has indeed proven fruitful, the superior healing precedent set by the seminal Grubbs' catalyst should disallow it from being deemed impractical for self-healing applications simply due to economic considerations.

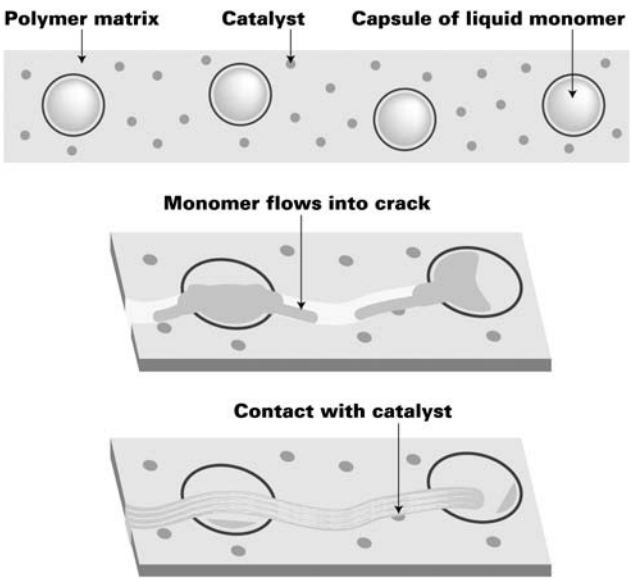

Fig. 1 Schematic representing self-healing of a polymer.

One approach to minimize the economic obstacle of using Grubbs' catalyst is to reduce the amount of catalyst required to achieve maximum healing potential. Unfortunately, efficient use of the catalyst in a self-healing system is often difficult due to the fact that the monomer needs to dissolve the catalyst in a very non-ideal mixing scenario; that is, elevated temperatures or external agitation cannot realistically be applied to aid catalyst dissolution during the healing event. In addition, sluggish catalyst dissolution can also likely be attributed to the fact that the catalyst particle is embedded in the crack surface, limiting the surface area of catalyst exposed to the liquid monomer during healing to one cross-sectional area of the particle. Nevertheless, others have developed rather clever techniques to promote efficient use of Grubbs' catalyst during healing. For example, Rule *et al.* showed that by first encapsulating Grubbs' catalyst particles in wax microspheres, a 10-fold decrease in catalyst loading can achieve similar or better healing relative to the original, wax-free self-healing systems.[22] Catalyst was used more efficiently due to the catalyst particles being smaller in size in the wax microspheres, which increases the surface area of catalyst exposed to liquid monomer. Furthermore, the Grubbs' catalyst was protected by the wax casing from surface layer decomposition caused by contact with the polymer matrix resin during composite fabrication. Another approach to more efficiently use catalyst is to incorporate different healing monomers and

[a]*Department of Chemistry, Iowa State University, Ames, IA, 50011, USA*
[b]*Department of Materials Science and Engineering, Iowa State University, 2220 Hoover Hall, Ames, IA, 50011, USA. E-mail: mkessler@iastate.edu*
† Electronic supplementary information (ESI) available: Density and molar volume values for the Healing Agent Library and the calculation of Beerbower group contributions and Hansen Parameters for norbornene. See DOI: 10.1039/c0jm00521e

monomer blends that inherently require less catalyst to achieve a high degree of polymerization, and therefore require lower loadings of catalyst in the self-healing polymer. For example, Liu *et al.* have identified a low viscosity, highly reactive ROMP monomer called ethylidene norbornene that can be used either neat or in blends with DCPD to, among other things, significantly reduce the required catalyst loading in a self-healing polymer.[23–27]

An alternate approach to efficiently using the catalyst in a self-healing polymer is to increase the rate at which catalyst is dissolved into the liquid monomer. Presumably, the reason why such a large amount of Grubbs' catalyst, relative to DCPD, is necessary in self-healing polymers is because the catalyst particles exposed on the crack surface are not entirely dissolved before DCPD undergoes appreciable amounts of polymerization, and therefore cannot easily dissolve more catalyst. Hence, the effective catalyst concentration is considerably lower than the feed concentration that is initially added to the self-healing polymer. So to reach maximum healing capabilities, comparatively large amounts of catalyst are necessary. Increasing the dissolution rate of the catalyst would then cause the effective concentration to approach the feed catalyst concentration, thus requiring less overall catalyst to achieve similar levels of healing. Jones *et al.* attempted to increase dissolution kinetics by grinding, freeze-drying, and recrystallizing catalyst particles to smaller sizes, thereby increasing their surface area.[28] Smaller catalyst particles were shown to dissolve faster in the healing monomer than the large, as-received Grubbs' catalyst particles. In some cases, this faster dissolution also improved healing by ensuring a relatively even distribution of dissolved catalyst throughout the monomer, which led to a continuous polymer film in the crack volume. This was unlike early self-healing systems with large, slow-dissolving catalyst particles, whose reaction with monomer was largely heterogeneous, leading to intermittent patches of polymer surrounding catalyst embedded in the crack plane. However, reducing catalyst particle size and increasing catalyst surface area are not without drawbacks. For example, as mentioned above, the extent of catalyst surface layer decomposition is increased with a greater surface area, and the smaller size potentially leads to catalyst dissolution in the polymer matrix resin in which it is embedded.

In addition to decreasing the amount of catalyst required for self-healing polymers, improving the bulk catalyst dissolution kinetics can also increase the speed of healing, which greatly expands self-healing polymer's potential application base. Ideally, self-repair should be as rapid as possible, especially for applications where the polymer may be subject to rapid or periodic stress. But it was recently observed that healing kinetics is not a simple phenomenon and dependent on many factors, notably the sensitive interplay between catalyst dissolution kinetics and bulk polymerization kinetics of the healing monomer.[29] In particular, it was noted that the bulk polymerization kinetics of the healing monomer should not greatly exceed the catalyst dissolution kinetics. Otherwise the system would result in a polymer with poor properties and "spotty" healing, similar to the aforementioned case of healing with large, slow-dissolving catalyst particles. Thus, catalyst dissolution kinetics is a significant (but often ignored) consideration when determining the speed and quality of self-healing.

In this paper, we create a small library of healing monomers and develop a model to make predictions regarding their ability to dissolve a catalyst in a self-healing polymer. While we anticipate our model can be versatile enough to be applicable to any type of healing chemistry, due to the robust and well-studied healing performance of ROMP-based self-healing, we focus our discussion here only on the dissolution of Grubbs' catalyst in ROMP-active healing monomers. In order to create this model, we borrow several ideas from the concept of solubility parameters, otherwise widely known in the realm of polymer physics as a means to make predictions regarding solute–solvent interactions and the thermodynamics of polymer mixing.[30] Details of the calculations and the strengths and limitations of the model are discussed in detail. And finally, the model is experimentally validated by directly measuring the dissolution rate of a structurally modified Grubbs' catalyst in various monomers and monomer blends. The structurally modified catalyst was used to inhibit polymerization of the ROMP-active monomers during the course of the dissolution.

Experimental

General considerations

Bis(tricyclohexylphosphine)benzylidene ruthenium dichloride (1st generation Grubbs' catalyst), bicyclo[2.2.1]hept-2-ene (norbornene), dicyclopentadiene, 5-vinyl-2-norbornene, 5-ethylidene-2-norbornene, 5-norbornene-2-carboxylic acid, 5-norbornene-2-methanol, tetramethylsilane, ethyl vinyl ether, and all solvents/starting materials/reagents used for synthesis were purchased from Aldrich and, unless stated otherwise, used as-received. While determining Grubbs' catalyst's parameters, all solvents known to not readily absorb atmospheric moisture were used as-received from freshly opened bottles. All other solvents were either purchased anhydrous or dried accordingly and were handled under a nitrogen gas purge. 5-Norbornene-2-carboxaldehyde,[31] 2-(chloromethyl)-5-norbornene,[32] 2-(bromomethyl)-5-norbornene,[33] ethyl 5-norbornene-2-carboxylate,[34] 5-(methoxymethyl)-2-norbornene,[35] and 2-acetyl-5-norbornene[36] were synthesized according to literature procedures. All 5-substituted norbornenyl-derivatives, either purchased or synthesized, were obtained as a mixture of *exo*- and *endo*-isomers. All other syntheses are described below. ^{1}H NMR spectra were recorded at either 300 or 400 MHz with a Varian Spectometer (Palo Alta, CA) using $CDCl_3$ as a solvent and residual chloroform as an internal reference. HR-MS was done on a Finnigan TSQ700 mass spectrometer (San Jose, CA). Unless otherwise stated, room temperature is defined as 23–24 °C.

Synthesis of phenyl vinyl ether

A modified version of the original preparation[37] was used. β-Bromophenetole (15 g, 75 mmol) was added to KOH (20 g, 0.36 mol), which had been ground into a fine powder. The suspension was heated to a reflux (~150 °C) for 12 hours. The crude product was isolated by vacuum filtration and purified by silica gel column chromatography (hexanes) to yield a clear, colorless liquid (3.1 g, 35%). ^{1}H NMR (300 MHz, $CDCl_3$): δ ppm 7.35 (apparent t, $J = 9$ Hz, 2H), 7.10 (t, $J = 9$ Hz, 1H), 7.04 (d, $J = 9$ Hz, 2H), 6.68 (dd, $J = 6$, 15 Hz, 1H), 4.79 (dd, $J = 3$, 15 Hz,

1H), 4.45 (dd, J = 3, 6 Hz, 1H). High-resolution mass spectrometry (HRMS) expected 120.0575, found 120.0571.

Synthesis of $(PCy_3)_2Cl_2Ru{=}C(H)OPh$

Phenyl vinyl ether (2.5 g, 21 mmol) was slowly added to a CH_2Cl_2 (10 ml) solution of Grubbs' 1st generation catalyst, $(PCy_3)_2Cl_2Ru{=}C(H)Ph$ (2 g, 2.4 mmol). This solution was allowed to stir at room temperature for 30 minutes, during which time the purple solution changed to a dark red color. The solvent was evaporated *in vacuo*, and the resulting solid was washed with 4 × 10 ml of cold (−25 °C) pentane to reveal a red solid (1.90 g, 93%). ^{1}H NMR (300 MHz, $CDCl_3$): δ ppm 14.84 (s, 1H), 7.36 (apparent t, J = 7.8 Hz, 2H), 7.21 (t, J = 7.5 Hz, 1H), 7.09 (d, J = 7.8 Hz, 2H), 2.72–2.64 (m, 6H), 2.01–1.97 (m, 12H), 1.81–1.71 (m, 19H), 1.61–1.51 (m, 13H), 1.35–1.20 (m, 16H). High resolution mass spectrometry (HRMS) expected 838.3479, found 838.3484.

Synthesis of *N*,*N*-dimethyl-5-norbornene-2-carboxamide

N,*N*-Dimethylacrylamide (15 g, 0.15 mol) was added to 250 ml ethyl acetate. Over the course of 30 minutes, freshly distilled cyclopentadiene (11 g, 0.17 mol) was added dropwise. After complete addition, the solution was brought to a gentle reflux and allowed to stir for 5 days in the dark, with an additional 1 ml of cyclopentadiene being added daily. Complete consumption of *N*,*N*-dimethylacrylamide was observed by silica gel thin-layer chromatography (ethyl acetate, R_f = 0.6), and volatiles were removed *in vacuo*. The resulting crude product was cooled to ~5 °C and triturated three times with pentane (1 × 250 ml, 2 × 100 ml). Upon warming to room temperature, a dark brown, viscous liquid was isolated (19.5 g, 78%) with sufficient purity (>95%). Product was a mixture of *endo*/*exo*-isomers (~4/1). ^{1}H NMR (300 MHz, $CDCl_3$) for the *endo*-isomer: δ ppm 6.15 (dd, J = 3.0, 5.7 Hz, 1H), 6.02 (dd, J = 3.0, 5.7 Hz, 1H), 3.10–3.01 (m, 2H), 3.07 (s, 3H), 2.90–2.83 (m, 1H), 2.88 (s, 3H), 1.97–1.89 (m, 1H), 1.41–1.32 (m, 2H), 1.28 (apparent d, J = 8.1 Hz, 1H). High-resolution mass spectrometry (HRMS) expected 165.1154, found 165.1160.

Dissolving Grubbs' catalyst in solvent

5 mg of Grubbs' 1st generation catalyst were weighed into a small, flame-dried vial, and the catalyst particles were evenly distributed throughout the bottom area of the vial. A given solvent was added to the vial *via* syringe (0.5 ml). The solvent addition was rapid enough to quickly cover the catalyst layer, but not so rapid that the even distribution of the catalyst along the bottom of the vial was disturbed. For those solvents whose saturation point was not reached after dissolving the 5 mg of catalyst (*i.e.* solubility of catalyst in solvent >5 mg per 0.5 ml), the approximate time for complete dissolution was recorded. For solvents that became saturated prior to completely dissolving the 5 mg catalyst, the saturation level was determined, and a similar dissolution experiment was rerun with half the amount of catalyst that can saturate the solvent (*e.g.* if the saturation level of Grubbs' catalyst in a solvent was determined to be 4 mg catalyst per 0.5 ml solvent, the subsequent dissolution test was done with 2 mg catalyst in 0.5 ml solvent). Three dissolution experiments were performed with each solvent. Each solvent's dissolution rate was categorized as either rapid, moderate, slow or deficient, based on Table 1:

Table 1 Ranking system for dissolution of Grubbs' catalyst in various solvents

Category	Description
Rapid	Fully dissolved during, or within a few seconds after, solvent addition
Moderate	30–90 seconds
Slow	2–5 minutes
Deficient	>5 minutes

Additionally, an extra dissolution experiment was performed with double the amount of each solvent in order to determine the dependence of the dissolution rate on the degree of undersaturation.

Dissolving Grubbs' catalyst in monomer

250 ± 1 mg of modified Grubbs' 1st generation catalyst, $(PCy_3)_2Cl_2Ru{=}C(H)OPh$, were weighed into a flame-dried vial, and the catalyst particles were evenly distributed throughout the area of the bottom of the vial. Exactly 5 ml of monomer or monomer blend containing 0.2 ml tetramethylsilane internal standard were quickly added to the catalyst in a manner that did not disturb the even distribution of catalyst on the bottom of the vial. At 5 minute intervals up to 30 minutes, 0.1 ml of liquid was withdrawn from the center of the solution. To these aliquots were added 10 μl of ethyl vinyl ether to ensure minimal or no polymerization during further characterization. ^{1}H NMR spectra (400 MHz, $CDCl_3$, 64 scans) were taken of the aliquots, and the amount of dissolved catalyst is defined as the molar ratio of catalyst to TMS internal standard, denoted herein as "relative intensity." Relative intensity was calculated by

$$\text{Relative intensity} = \frac{\sum I_{Ru=C(H)R}}{I_{TMS}/12} \quad (1)$$

where $\Sigma I_{Ru=C(H)R}$ is the sum of all ruthenium carbene integrations, and I_{TMS} is the integration value of tetramethylsilane. Reported relative intensity values are the average of three dissolution experiments.

Results and discussion

Healing monomer library dissolution parameters

For each monomer in the healing monomer library (shown in Fig. 2) we calculated a set of Hansen parameters, which were

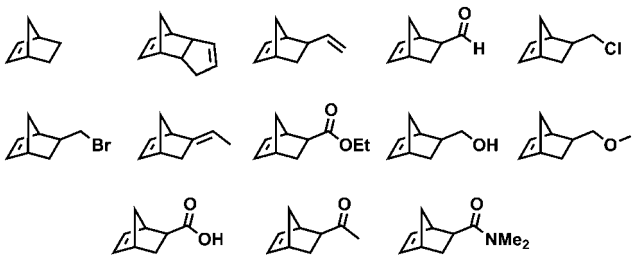

Fig. 2 ROMP-active, healing monomer library.

originally developed to provide a semi-quantitative model for predicting cohesive compatibility between solvents, plasticizers, polymers, dyes, *etc.*[38] Hansen parameters, denoted as δ_x, are defined as the square root of the cohesive energy density related to an x-type intermolecular attraction, where chemicals with similar parameters have both similar cohesive energies and, more importantly for the present work, greater chemical compatibility. A conceptual explanation of Hansen parameters and their calculation is discussed briefly here, and in much greater detail in ref. 39.

A Hansen parameter of a chemical's x-type cohesive force can be directly calculated from the x-type force's contribution to the total cohesive energy of a chemical, E_x, normalized by its molar volume, V:

$$\delta_x = \sqrt{\frac{E_x}{V}} \quad (2)$$

There are three parameters historically defined as Hansen parameters: δ_D, the parameter related to intermolecular dispersion forces; δ_P, the parameter related to fixed-dipole forces; and δ_H, a parameter classically known as the hydrogen-bonding parameter, but often regarded as an electron-transfer parameter. As shown in eqn (3), the sum of the squares of the Hansen parameters is equivalent to the total parameter, δ_T, which is known as the one-dimensional, Hildebrand parameter. Additionally, using eqn (2) and (3), the relationship can be rewritten directly as a function of cohesive energy densities (eqn (4)), although dealing with the smaller Hansen parameters is often more convenient.

$$\delta_T^2 = \delta_D^2 + \delta_P^2 + \delta_H^2 \quad (3)$$

$$\frac{E_T}{V} = \frac{E_D}{V} + \frac{E_P}{V} + \frac{E_H}{V} \quad (4)$$

Then, chemicals with similar parameters can be considered chemically compatible and have some favorable intermolecular interactions. While Hansen parameters are most often used to make predictions regarding thermodynamic-based interactions of two or more chemicals (*e.g.* solubility, polymer swelling in a solvent, polymer mixing, *etc.*), it has been shown that they can also potentially be useful in linking together chemicals' kinetic processes,[40] but to the best of our knowledge, have never been used to make predictions on dissolution. However, it should be noted that these parameters are only meant to be a useful guide for making predictions, and their specific values should be considered approximations that cannot predict minor differences in behavior.

While Hansen parameters can be calculated experimentally, reasonably accurate values can be obtained using the Beerbower group contribution method, where atomic groups (*e.g.* –CH_2–, =CH–, –OH, –C_6H_5, –NH_2, *etc.*) have fixed cohesive energy contributions related to a specific Hansen intermolecular force (*i.e.* dispersion, fixed-dipole or hydrogen-bonding). Lists of the Beerbower group contributions can be found in numerous sources.[39] In order to determine E_x for a given chemical, the sum of the appropriate atomic group contributions for that chemical is determined, and the corresponding Hansen parameters are calculated using eqn (2). However, our initial efforts to directly use this group contribution approach were unsuccessful,

Table 2 Complete Hansen parameters for the healing monomer library

Monomer[a]	δ_T	δ_D	δ_P	δ_H
–H	16.0	15.5	1.4	3.7
–CH=CH–CH_2–	17.8	17.1	1.8	4.7
–CH=CH_2	16.2	15.4	1.7	4.6
=CH–CH_3	16.7	15.9	2.0	4.7
–COOEt	16.9	15.3	3.2	6.4
–CH_2–OH	22.9	18.0	5.1	13.2
–COOH	21.4	18.5	3.5	10.3
–$COCH_3$	19.3	17.5	5.7	6.0
–CHO	20.4	16.1	10.4	6.9
–CH_2–Cl	18.2	16.7	6.3	3.7
–CH_2–Br	18.5	16.7	6.2	5.0
–CH_2–O–CH_3	16.9	15.7	3.9	4.8
–$CON(CH_3)_2$	22.7	18.5	9.8	8.8

[a] The functional group listed refers to a derivative of 2-norbornene functionalized with this group at the 5-position.

presumably a result of the norbornenyl functionality present on all of our healing monomers being a highly strained, bicyclic structure, while group contributions are generally intended for use with small, linear, and strain-free molecules. Hence, we experimentally calculated the "atomic group contribution" for the 2-norbornenyl-group with covalent connectivity at the 5-position (the functionalized position in the majority of our 2-norbornenyl-based library). Then, our 2-norbornenyl "group contribution" was used concurrently with the Beerbower group contributions to build Hansen parameters for our healing monomer library. Further details regarding the calculation of the 2-norbornenyl "group contribution" are available in the ESI† for this paper, and the full set of Hansen parameters for all healing monomers is shown in Table 2.

The parameters for the healing monomer library are shown in Fig. 3, expressed as a 2-dimensional Hansen Parameter Map, which we refer to as a Healing Monomer Map. Since the δ_D Hansen parameters for all of the healing monomers are very similar (16.7 ± 1.1 $MPa^{1/2}$), they are intentionally ignored both in

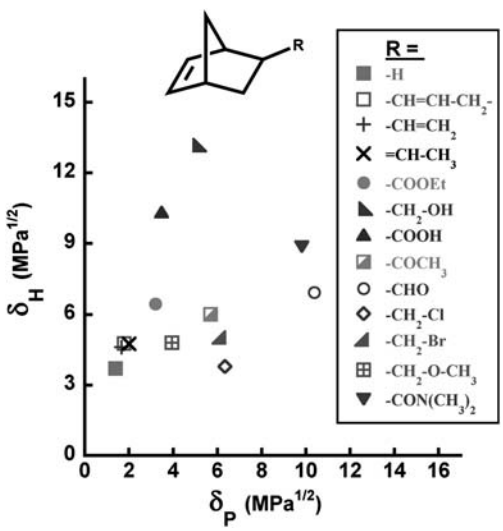

Fig. 3 Healing Monomer Map for the ROMP-active library used in this study.

Fig. 3 and when comparing the parameters of different chemicals (*vide infra*), which is commonly done with Hansen parameters. It is noteworthy that, for all healing monomers, $\delta_H > 3$. This is true even for the hydrocarbon monomers that are not expected to show significant hydrogen bonding. But as mentioned above, the "hydrogen-bonding" parameter nomenclature is something of a misnomer, used largely due to historical precedent, and instead should be considered as a parameter related to electron-transfer intermolecular forces. Therefore, the unexpectedly large δ_H values can be explained by the norbornenyl-group's double bond acting as a Lewis base, which is essentially defined as a species that can undergo electron-transfer. Furthermore, the Lewis basicity of the norbornenyl double bond is especially high, relative to other double bonds, because donation of its π-bonding electrons would result in a moderate relief of ring-strain in the highly strained norbornenyl functionality. All other Hansen parameters for the healing monomers fall within expected ranges for the functional groups on each monomer (*i.e.* hydrocarbons have low δ_P values, the amide has a high δ_P value, monomers with a removable hydrogen have high δ_H values, *etc.*).

Catalyst dissolution parameters

The Hansen parameters for Grubbs' Catalyst were determined by qualitatively measuring dissolution of the catalyst in various common organic solvents with well known parameters. A total of 34 solvents with a wide array of Hansen parameters were chosen (Hansen parameters for common solvents can be found in numerous sources, for example ref. 39), which are plotted in Fig. 4a. While it was difficult to quantify dissolution rate of the catalyst in the solvents for a variety of reasons (some extremely rapid dissolution, some extremely slow dissolution, and an overall great deal of scatter in quantitative measurements), it was surprisingly easy and reliable to qualitatively determine dissolution rates. Dissolution rates of the catalyst in the solvents naturally fell into four categories, which we denote herein as rapid, moderate, slow and deficient (Fig. 4b), which are described in more detail in the experimental section of this paper. Assignment of the solvents into these four categories was straightforward, and very few solvents were at the "borderline" of two categories, but any type of ranking of the solvents within each category is futile due to the amount of scatter during attempts to quantify dissolution. On a side note, several of the solvents used in this study are known to react with Grubbs' catalyst (*e.g.* acetonitrile, acrylonitrile, aniline, pyridine, piperidine and pyrrole), and can potentially skew their inherent dissolution kinetics. However, we found that our interpretation of the Hansen Parameter Map both including and excluding the data points accrued from these solvents was essentially identical.

During dissolution measurements, which are described in more detail in the experimental section of this paper, temperature (room temperature), agitation rate (no agitation), and interfacial area of the catalyst available to the monomer were kept constant, forcing the dissolution rate to be dependent solely on chemical compatibility between the solvents and the catalyst. However, one potential concern while taking dissolving measurements is that the degree of undersaturation may affect the dissolution rate. But increasing the amount of solvent available to dissolve the catalyst, which would increase the degree of undersaturation, seemed to have minimal effect on the dissolution. At the very least, the different degrees of undersaturation did not create ambiguity as to which of the four qualitative dissolution categories the solvents should be placed.

It is clear from Fig. 4b that there are localized regions of rapid, moderate, slow and deficient dissolution on the Hansen Parameter Map; the regions of rapid dissolution are marked by arrows. Additionally, the regions of rapid dissolution seem to be roughly circular in shape, and proceeding outside the "rapid" dissolving circle are sequential regions of moderate, slow, and deficient dissolution. This is consistent with what is observed for polymers, which commonly have "spheres" on their Hansen Parameter Maps that correspond to regions of good solubility, swelling, *etc.* in solvents whose parameters are within the "sphere," and the center coordinates of the "sphere" correlates to the polymer's Hansen parameters.[39] While the existence of multiple spheres, as in this work, is very uncommon with polymers, there is some precedent for multiple spheres in a Hansen Parameter Map for other organometallic compounds.[41] Therefore, we confidently assign Grubbs' catalyst two sets of Hansen parameters, which are roughly calculated to be ($\delta_P = 2.9$, $\delta_H = 3.3$) and ($\delta_P = 7.0$, $\delta_H = 7.1$).

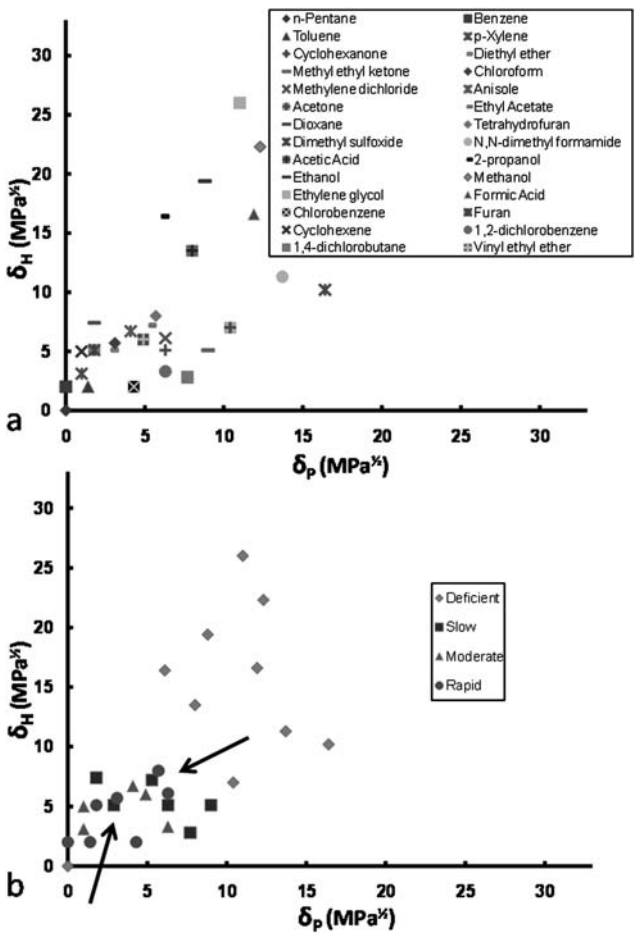

Fig. 4 (a) Solvent parameter map and (b) results of dissolution measurements of Grubbs' catalyst in each solvent. The arrows denote regions of superior dissolution.

Table 3 Hansen parameters for three healing monomers and their volume fractions required to make a blend that approximately matches one of the Hansen parameters of the Grubbs' catalyst ($\delta_P = 2.9$, $\delta_H = 3.3$). The "R =" corresponds to the functional group at the 5-position of the norbornenyl-based monomer

	Volume fraction				
Entry	R = H	R = COOEt	R = $COCH_3$	δ_P/MPa$^{1/2}$	δ_H/MPa$^{1/2}$
1[a]	1	0	0	1.4	3.7
2	0	1	0	3.2	6.5
3	0	0	1	5.7	6.0
4	0.62	0.06	0.32	2.9	4.6

[a] Test conducted at ~50 °C.

Model validation

By comparing Fig. 3 and 4b, it is apparent that no healing monomer's Hansen parameters coincide very well with Grubbs' catalyst's parameters, implying that the maximum dissolution kinetics cannot be achieved with a one-component healing monomer. However, Hansen parameters are known to obey a simple rule of mixing; in other words, any miscible blend of liquids takes on the Hansen parameters intermediate between the separate components of the blend,[39] as shown in eqn (5).

$$\delta_{x,\text{blend}} = \sum \theta_i \delta_{x,i} \quad (5)$$

In this equation, $\delta_{x,\text{blend}}$ is the Hansen parameter of the x-type cohesive force (*i.e.* Dispersion, Dipole or Hydrogen bonding forces) in the blend of liquids, θ_i is the volume fraction of the i-th liquid in the blend, and $\delta_{x,i}$ is the Hansen parameter of the x-type cohesive force for the i-th liquid in the blend. Therefore, to experimentally validate our model, various healing monomers were blended in the appropriate volume fractions that would cause the blend to have Hansen parameters similar to the catalyst's parameters. The two healing monomer blends chosen for this study (one blend to match each of the Grubbs' catalyst's two Hansen parameters) are shown in Tables 3 and 4. It should be noted that the blend represented in Table 3 (Hansen parameters: ($\delta_P = 2.9$, $\delta_H = 4.6$)) does not exactly match the estimated Hansen parameters of Grubbs' catalyst ($\delta_P = 2.9$, $\delta_H = 3.3$). This is because this set of Grubbs' catalyst parameters falls out of the range of the parameters of our healing monomer library, making it mathematically impossible to find a monomer blend that precisely matches the catalyst's parameters. Hence, a blend was chosen whose overall Hansen parameters are reasonably close to that of the Grubbs' catalyst; possible errors resulting from this modification are discussed below.

Table 4 Hansen parameters for three healing monomers and their volume fractions required to make a blend that matches one of the Hansen parameters of the Grubbs' catalyst ($\delta_P = 7.0$, $\delta_H = 7.1$). The "R =" corresponds to the functional group at the 5-position of the norbornenyl-based monomer

	Volume fraction				
Entry	R = COOH	R = CHO	R = CH_2Br	δ_P/MPa$^{1/2}$	δ_H/MPa$^{1/2}$
1	1	0	0	3.5	10.3
2	0	1	0	10.4	6.9
3	0	0	1	6.2	5.0
4	0.27	0.36	0.37	7.0	7.1

An obvious problem with measuring the dissolution rate of Grubbs' catalyst with a ROMP-reactive monomer is the ensuing polymerization reaction affecting dissolution. While the dynamic structural and rheological environment resulting from bulk polymerization is indeed indicative of what is actually occurring during the complex self-healing process, for the purposes of this study where we focus solely on dissolution rates (and need a suitable method to measure dissolution), the polymerization reaction must be temporarily stopped. To achieve this, a modified version of Grubbs' catalyst with extremely low ROMP-reactivity was synthesized (shown in Fig. 5 along with the structure of the Grubbs' catalyst). While this catalyst is not exactly inactive, the placement of an oxygen atom between the carbene and the phenyl group places the catalyst into a thermodynamic well, which was sufficient to inhibit an appreciable amount of polymerization in the time-scale of our experiments. In fact, for other alkoxy carbene-derivatives of Grubbs' catalyst, this ROMP-inhibition was observed for higher catalyst concentrations, longer times, and higher temperatures than those in this study.[42] Of course, this structural modification should not come at the expense of significantly changing the Hansen parameters of the catalyst. Thus, dissolution tests of the modified catalyst in solvent similar to those described in the previous section were done, which yielded similar results as the unmodified catalyst.

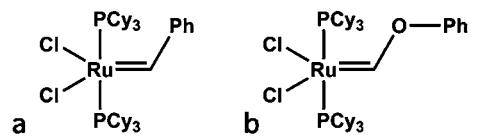

Fig. 5 (a) Grubbs 1st generation catalyst and (b) a ROMP-inactive, modified version of Grubbs' catalyst.

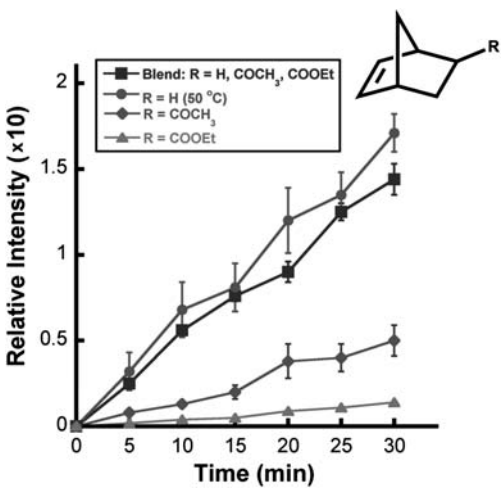

Fig. 6 Dissolution of a modified Grubbs' catalyst in various monomers and monomer blends. The "R =" group in the legend denotes the functionality at the 5-position of the norbornenyl group. The monomer blend has Hansen parameters of ($\delta_P = 2.9$, $\delta_H = 4.6$), which is similar to that of the catalyst.

Therefore the modified Grubbs' catalyst shown in Fig. 5 was used in all dissolution tests of catalyst in healing monomer.

Ideally, monomers and monomer blends with parameters closer to the catalyst's parameters would dissolve the catalyst fastest. NMR-based dissolution tests (see Experimental section) of the first monomer blend ($\delta_P = 2.9$, $\delta_H = 4.6$; shown in Table 3) and the individual components of this blend are shown in Fig. 6. As mentioned earlier, it was not possible to construct a monomer blend with Hansen parameters that equaled the catalyst's first set of parameters, so the blend in Table 3 was chosen as having parameters close to the catalyst; at the very least, the blend's parameters were closer to the catalyst than any of the components of the blend. As seen in Fig. 6, the dissolution rate of the catalyst by the blend and by norbornene (R = H) were approximately equal, followed by the acetyl-functionalized norbornenyl derivative (R = $COCH_3$) and the ester-functionalized derivative (R = COOEt). However, it is important to note that because norbornene is a solid at room temperature, its dissolution experiments had to be carried out at elevated temperatures (~50 °C). Although it is hard to distinguish differences in the dissolution rates of the blend and of norbornene from experimental error, it is definitely reasonable to presume that norbornene's theoretical room temperature dissolution rate would be slower than that of the blend, which is in agreement with our model predictions. Furthermore, the proximity of norbornene's Hansen parameters to the catalyst is not too dissimilar from the proximity of the blend's parameters to the catalyst. So even if the reduction in norbornene's dissolution rate from ~50 °C to room temperature was small enough to still be indistinguishable from that of the blend, our model would still predict dissolution behavior reasonably well. The slower dissolution rates of the acetyl and ester-functionalized norbornenyl groups are also in agreement with predictions—both monomers have Hansen parameters that are, comparably, far from that of the catalyst. In fact, the catalyst's parameters ($\delta_P = 2.9$, $\delta_H = 3.3$) are slightly closer to that of the acetyl-functionalized derivative than the ester-derivative. This predicts that the dissolution rate of the catalyst by the acetyl-derivative would be slightly faster than the ester, which is also in agreement with what is experimentally observed.

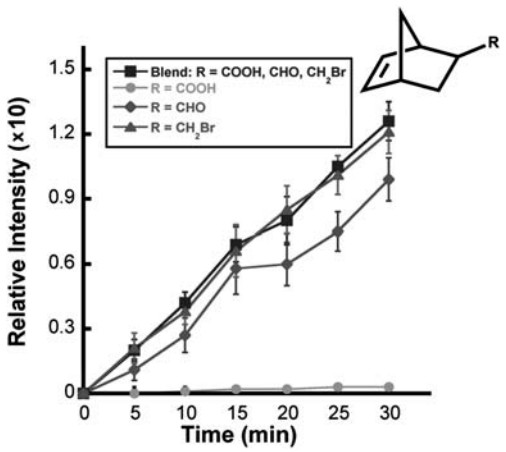

Fig. 7 Dissolution of a modified Grubbs' catalyst in various monomers and monomer blends. The "R =" group in the legend denotes the functionality at the 5-position of the norbornenyl group. The monomer blend has Hansen parameters of ($\delta_P = 7.0$, $\delta_H = 7.1$), which matches that of the catalyst.

A blend whose Hansen parameters matched the second set of Grubbs' catalyst's parameters ($\delta_P = 7.0$, $\delta_H = 7.1$) was constructed from three of the healing monomers, which are shown in Table 4. Dissolution experiments of the modified Grubbs' catalyst with this blend and the individual components of the blend were conducted, and this data is shown in Fig. 7. The acid-functionalized norbornenyl-derivative (R = COOH) was obviously the slowest to dissolve the catalyst, which is expected from the large distance of the acid's Hansen parameters from that of the catalyst. The aldehyde-functionalized monomer (R = CHO) was much faster to dissolve the catalyst than the acid, but slower than both the blend and the bromomethyl-functionalized norbornene (R = CH_2Br). This is also predicted with our Hansen parameter-based model, as the aldehyde-derivative's Hansen parameters are closer to the catalyst's parameters than the acid, but further than both the blend and the bromomethyl-derivative. However, the dissolution rates of the catalyst by the blend and the bromomethyl-norbornene monomer are nearly identical. The Hansen parameters of the bromomethyl-derivative are closer to the catalyst's parameters than almost all of the other components in the healing monomer library, so a relatively rapid dissolution rate is expected, but the fact that it has a dissolution rate as rapid as the blend (which exactly matches the catalyst's parameters) falls outside of what is expected with our model. There are several possible explanations for this behavior. First, the possibility that the second set of Grubbs' catalyst Hansen parameters ($\delta_P = 7.0$, $\delta_H = 7.1$) is not entirely accurate cannot be ignored. As mentioned earlier, Hansen parameters are a semi-quantitative technique in that the large degree of error in their calculation makes it difficult to predict minor differences in behavior. Perhaps the difference in the proximities of the parameters between the catalyst/blend and the catalyst/bromomethyl-derivative is too small, thereby causing the inaccuracies in parameter calculations to become more evident. But the most likely explanation for the blend's dissolution rate being closer than expected to the bromomethyl-derivative's dissolution rate is viscosity. Dissolution rates are known to be viscosity-dependant,[43] with trends of generally slower dissolution with increasing viscosity. It is easily observed that the blend, which contains 27% of the highly viscous acid-functionalized norbornene, is of a higher viscosity than the bromomethyl norbornenyl-derivative. Hence, it is reasonable to assume that the blend's rate of dissolving catalyst is being effectively reduced as a result of its higher viscosity, and the model predictions were not necessarily incorrect. Nonetheless, it should be noted in future utilizations of this model that dissolution rates will probably fall short of Hansen parameter-based predictions when using healing monomers of higher viscosities. While this is indeed a limitation of using the model presented here, most of the healing monomers in the library of Fig. 1 were liquids of relatively low viscosity. In fact, this viscosity effect probably has not manifested itself in the other experiments presented in this paper because all of the other healing monomers tested have similar viscosities, at least by visual inspection. Furthermore, high-viscosity healing monomers and monomer blends are already considered unfavorable for self-healing for a number of reasons, and they would therefore likely

be prematurely excluded as a possibility when considering a feasible healing monomer/catalyst combination.

Conclusion

In this paper, a model was developed using the concept of Hansen parameters in order to make predictions regarding the dissolution of a solid catalyst in liquid monomers for self-healing applications. More specifically, we developed our model in reference to the dissolution of Grubbs' catalyst in a library of ROMP-active monomers, which are often used as a catalyst/healing monomer combination in other self-healing works. Hansen parameters were calculated for a small library of norbornenyl-based monomers, which are generally reactive *via* the ROMP reaction. The Grubbs' catalyst was found to have two sets of Hansen parameters, and blends of healing monomers created to match these parameters were found to dissolve the catalyst rapidly. However, the model is limited in its ability to predict and compare dissolution rates of liquids with significantly different viscosities. While our model was developed for a ROMP-based self-healing system, we believe this Hansen parameter technique is fundamental and versatile enough to be applied to other types of self-healing chemistries.

Acknowledgements

This work was supported by The American Chemical Society Petroleum Research Fund (ACS PRF# 47700-AC7). The authors gratefully acknowledge Dr Xia Sheng, Dr Wonje Jeong, and Dr Malika Jeffries-EL for helpful discussions.

References

1 M. R. Kessler, Self-healing: a new paradigm in materials design, *Proc. Inst. Mech. Eng., Part G*, 2007, **221**(4), 479–495.
2 R. P. Wool, Self-healing materials: a review, *Soft Matter*, 2008, **4**, 400–418.
3 S. D. Bergman and F. Wudl, Mendable polymers, *J. Mater. Chem.*, 2008, **18**, 41–62.
4 S. R. White, N. R. Sottos, P. H. Geubelle, J. S. Moore, M. R. Kessler, S. R. Sriram, E. N. Brown and S. Viswanathan, Autonomic healing of polymer composites, *Nature*, 2001, **409**, 794–797.
5 M. R. Kessler, N. R. Sottos and S. R. White, Self-healing structural composite materials, *Composites, Part A*, 2003, **34**, 743–753.
6 K. S. Toohey, N. R. Sottos, J. A. Lewis, J. S. Moore and S. R. White, Self-healing materials with microvascular networks, *Nat. Mater.*, 2007, **6**, 581–585.
7 K. S. Toohey, C. Hansen, N. R. Sottos, J. A. Lewis and S. R. White, Delivery of two-part self-healing chemistry *via* microvascular networks, *Adv. Funct. Mater.*, 2009, **19**, 1399–1405.
8 E. L. Dias, S. T. Nguyen and R. H. Grubbs, Well-defined ruthenium olefin metathesis catalysts: mechanism and activity, *J. Am. Chem. Soc.*, 1997, **119**, 3887–3897.
9 T. M. Trnka and R. H. Grubbs, The development of L2X2Ru=CHR olefin metathesis catalysts: an organometallic success story, *Acc. Chem. Res.*, 2001, **34**, 18–29.
10 C. W. Bielawski and R. H. Grubbs, Living ring-opening metathesis polymerization, *Prog. Polym. Sci.*, 2007, **32**, 1–29.
11 E. Kirkby, V. Michaud, J. A. Manson, J. D. Rule, N. R. Sottos and S. R. White, Embedded shape-memory allow wires for improved performance of self-healing polymers, *Adv. Funct. Mater.*, 2008, **18**, 2253–2260.
12 X. Sheng, J. K. Lee and M. R. Kessler, The influence of cross-link density on the properties of ROMP thermosets, *Polymer*, 2009, **50**, 1264–1269.
13 G. O. Wilson, J. S. Moore, S. R. White, N. R. Sottos and H. M. Andersson, *Adv. Funct. Mater.*, 2008, **18**, 44–52.
14 M. R. Kessler and S. R. White, Cure kinetics of ring-opening metathesis polymerization of dicyclopentadiene, *J. Polym. Sci., Part A: Polym. Chem.*, 2002, **40**, 2373–2383.
15 G. E. Larin, M. R. Kessler, N. Bernklau and J. C. DiCesare, Rheokinetics of ring-opening metathesis polymerization of norbornene based monomers intended for self-healing applications, *Polym. Eng. Sci.*, 2006, **46**, 1804–1811.
16 T. C. Mauldin and M. R. Kessler, Latent catalytic systems for ring-opening metathesis-based thermosets, *J. Therm. Anal. Calorim.*, 2009, **96**, 705–713.
17 M. R. Kessler and S. R. White, Self-activated healing of delamination damage in woven composites, *Composites, Part A*, 2001, **32**, 683–699.
18 S. H. Cho, H. M. Andersson, S. R. White, N. R. Sottos and P. V. Braun, Polydimethylsiloxane-based self-healing materials, *Adv. Mater.*, 2006, **18**(8), 997–1000.
19 Y. C. Yuan, M. Z. Rong, M. Q. Zhang, J. Chen, G. C. Yang and X. M. Li, Self-healing polymeric materials using epoxy/mercaptan as the healant, *Macromolecules*, 2008, **41**(14), 5197–5202.
20 M. M. Caruso, B. J. Blaiszik, S. R. White, N. R. Sottos and J. S. Moore, Full recovery of fracture toughness using a nontoxic solvent-based self-healing system, *Adv. Funct. Mater.*, 2008, **18**, 1898–1904.
21 X. Sheng, T. C. Mauldin and M. R. Kessler, *J. Polym. Sci., Part A: Polym. Chem.*, 2010, submitted.
22 J. D. Rule, E. N. Brown, N. R. Sottos, S. R. White and J. S. Moore, Wax-protected catalyst microspheres for efficient self-healing materials, *Adv. Mater.*, 2005, **17**, 205–208.
23 X. Liu, J. K. Lee, S. H. Yoon and M. R. Kessler, Characterization of diene monomers as healing agents for autonomic damage repair, *J. Appl. Polym. Sci.*, 2006, **101**, 1266–1272.
24 J. K. Lee, X. Liu, S. H. Yoon and M. R. Kessler, Thermal analysis of ring-opening metathesis polymerized healing agents, *J. Polym. Sci., Part B: Polym. Phys.*, 2007, **45**, 1771–1780.
25 X. Liu, X. Sheng, J. K. Lee, M. R. Kessler and J. S. Kim, Rheokinetic evaluation of self-healing agents polymerized by Grubbs' catalyst embedded in various thermosetting resins, *Compos. Sci. Technol.*, 2009, **69**, 2102–2107.
26 X. Liu, X. Sheng, M. R. Kessler and J. K. Lee, Isothermal cure characterization of ROMP healing agents for autonomic damage repair: the glass transition temperature and conversion, *J. Therm. Anal. Calorim.*, 2007, **89**, 453–457.
27 X. Liu, X. Sheng, J. K. Lee and M. R. Kessler, Synthesis and characterization of melamine–urea–formaldehyde microcapsules containing ENB-based self-healing agents, *Macromol. Mater. Eng.*, 2009, **294**, 389–395.
28 A. S. Jones, J. D. Rule, J. S. Moore, S. R. White and N. R. Sottos, Catalyst morphology and dissolution kinetics of self-healing polymers, *Chem. Mater.*, 2006, **18**, 1312–1317.
29 T. C. Mauldin, J. D. Rule, N. R. Sottos, S. R. White and J. S. Moore, Self-healing kinetics and the stereoisomers of dicyclopentadiene, *J.R. Soc., Interface*, 2007, **4**, 389–393.
30 J. Hildebrand and R. L. Scott, *The Solubility of Nonelectrolytes*, Reinhold, New York, 3rd edn, 1950.
31 P. V. Bonnesen, C. L. Puckett, R. V. Honeychuck and W. H. Hersh, Catalysis of Diels–Alder reactions by low oxidation state transition-metal Lewis acids: fact and fiction, *J. Am. Chem. Soc.*, 1989, **111**, 6070–6081.
32 P. K. Freeman, V. N. Mallikarjuna Rao, D. E. George and G. L. Fenwick, The reactions of *exo*- and *endo*-5-chloromethylnorbornene with sodium, *J. Org. Chem.*, 1967, **32**, 3958–3963.
33 S. J. Dolman, K. C. Hultzsch, F. Pezet, X. Teng, A. H. Hoveyda and R. R. Schrock, Supported chiral Mo-based complexes as efficient catalysts for enantioselective olefin metathesis, *J. Am. Chem. Soc.*, 2004, **126**, 10945–10953.
34 I. S. Ponticello, The preparation of α-substituted acrylic esters, *J. Polym. Sci., Polym. Chem. Ed.*, 1979, **17**, 3509–3518.
35 S. Oh, J.-K. Lee, P. Theato and K. Char, Nanoporous thin films based on polylactide-grafted norbornene copolymers, *Chem. Mater.*, 2008, **20**, 6974–6984.
36 P. Beslin, D. Lagain, J. Vialle and C. Minot, Preparation of α-unsaturated acyclic thioketones—regioselective dimerization of 4*H*-1,3-dithiin, *Tetrahedron Lett.*, 1981, **37**, 3839–3845.
37 W. M. Lauer and M. A. Spielman, Synthesis of α,β-unsaturated ethers, *J. Am. Chem. Soc.*, 1931, **53**, 1533–1536.

38 (*a*) C. M. Hansen, The three dimensional solubility parameter—key to paint component affinities I. Solvents, plasticizers, polymers, and resins, *J. Paint Technol.*, 1967, **39**, 104–117; (*b*) C. M. Hansen, The three dimensional solubility parameter—key to paint component affinities II. Dyes, emulsifiers, mutual solubility and compatability, and pigments, *J. Paint Technol.*, 1967, **39**, 505–510; (*c*) C. M. Hansen and K. Skaarup, The three dimensional solubility parameter—key to paint component affinities III. Independent calculation of the parameter components, *J. Paint Technol.*, 1967, **39**, 11–514.
39 C. M. Hansen, *Hansen Solubility Parameters: A User's Handbook*, CRC Press, Boca Raton, FL, 2nd edn, 2007.
40 A. F. M. Barton, Applications of solubility parameters and other cohesion parameters in polymer science and technology, *Pure Appl. Chem.*, 1985, **57**, 905–912.
41 Personal communication between Alan Beerbower and Charles Hansen, which revealed two distinct solubility spheres for lithium stearate (further details in ref. 39).
42 J. Louie and R. H. Grubbs, Metathesis of electron-rich olefins: structure and reactivity of electron-rich carbene complexes, *Organometallics*, 2002, **21**, 2153–2164.
43 U. V. Banakar, *Pharmaceutical Dissolution Testing*, Marcel Dekker, Inc., New York, 1992, vol. 49.

